THERMODYNAMIC ASSESSMENT OF S-CO_2 BRAYTON CYCLE INTEGRATED WITH CASCADED LIBR-H_2O AND TRANS-CO_2 VAS FOR WASTE HEAT RECOVERY OF GAS TURBINE ENGINE.

A DISSERTATION

SUBMITTED IN PARTIAL FULFILMENT OF THE REQUIREMENTS FOR THE AWARD OF THE DEGREE OF

MASTER OF TECHNOLOGY

In

Thermal Engineering

HARSH VERMA

(2K20/THE/11)

Under the supervision of

PROF.RAJESH KUMAR

Mechanical Engineering Department
Delhi Technological University

MECHANICAL ENGINEERING DEPARTMENT

DELHI TECHNOLOGICAL UNIVERSITY

Shahbad Daulatpur, Bawana Road

Delhi- 110042, INDIA

MAY, 2022

MECHANICAL ENGINEERING DEPARTMENT

DELHI TECHNOLOGICAL UNIVERSITY

(Formerly Delhi College of Engineering)

Bawana Road, Delhi- 110042

CERTIFICATE

I hereby certify that the Project Dissertation titled "**Thermodynamic assessment of S-CO_2 Brayton cycle integrated with cascaded libr-H_2O and Trans-CO_2 VAS for waste heat recovery of gas turbine engine.**" which is submitted by **Harsh Verma, 2K20/THE/11**, Department of Mechanical Engineering, Delhi Technological University, Delhi in partial fulfilment of the requirement for the award of the degree of Master of Technology, is record of the project work carried out by the student under my supervision. To the best of my knowledge this work has not been submitted in part or full for any Degree of Diploma to this University or elsewhere.

Place: Delhi

Date: 31/05/2022

PROF. RAJESH KUMAR

SUPERVISOR

MECHANICAL ENGINEERING DEPARTMENT

DELHI TECHNOLOGICAL UNIVERSITY

MECHANICAL ENGINEERING DEPARTMENT

DELHI TECHNOLOGICAL UNIVERSITY

(Formerly Delhi College of Engineering)

Bawana Road, Delhi- 110042

CANDIDATE'S DECALARATION

I **Harsh Verma**, 2K20/THE/11 student of M. TECH (Thermal Engineering), hereby declare that the project Dissertation titled "**Thermodynamic assessment of Supercritical CO_2 Brayton cycle integrated with cascaded Transcritical co_2 and LiBr-H_2O Vapour absorption system for waste heat recovery of Gas turbine**" which is submitted by me to the department of Mechanical Engineering, Delhi Technological University, Delhi in partial fulfilment of the requirement for the award of the degree of Master of Technology, is original and not copied from any source without proper citation. This work has not previously formed the basis for the award of any Degree, Diploma Associateship, Fellowship or other similar title or recognition.

Place: Delhi

Date: 31/05/2022 **HARSH VERMA**

ACKNOWLEDGEMENTS

I express my sincere gratitude to my supervisor **Prof. Rajesh Kumar** for assisting me in identifying and formulating the research problem. Despite their busy schedules, Prof. Rajesh Kumar was always available for the advice and discussions. His valuable comments and advice gave me the confidence to overcome the challenges in the formulation of this research work. Also, I would like to express my sincere gratitude to my parents for their endless inspiration, support, and guidance throughout my whole life. Furthermore, I would like to thank my friends from the Mechanical Engineering department, who have supported me through their encouragement, support and friendship during this period of research work. Lastly, I would like to thank all those who directly and indirectly helped me in carrying out this thesis work successfully.

HARSH VERMA

(2K20/THE/11)

ABSTRACT

With rising global oil costs and growing environmental consciousness, the power sector is grappling with how to enhance gas turbine efficiency and minimise pollutant emissions from gas turbines. Waste heat recovery is an efficient way to increase gas turbine fuel efficiency and assist future turbines satisfy the more demanding Energy Efficiency Design Standard. In the present study, thermodynamic modelling and analysis of waste heat recovery comprising of Supercritical Carbon Dioxide recompression Brayton cycle, Transcritical Carbon Dioxide cycle, water lithium bromide vapour absorption system has been proposed for Gas turbine application based on first and second law thermodynamic laws. Thermodynamic performance of standalone Supercritical Carbon Dioxide Recompression Brayton cycle was compared with the proposed Design on the basis of standard operating design conditions. For thermodynamic analysis of combined system, high temperature exhaust gas of Titan^{TM} 350 (Designed by Solar turbines-a Caterpillar company) was utilised. Energic efficiency of standalone SRBC was found to be 35.92 % while Exergic efficiency was found to be 60.26 %. The overall thermal efficiency of proposed cycle was found to be 40.37% which signifies that waste heat can be recovered efficiency when combination of cycles is used. It was also found that the variation of important parameters such as compressor inlet temperature, turbine inlet temperature, and pressure ratio have a significant effect on the performance on standalone supercritical carbon dioxide recompression Brayton cycle.

List of Abbreviations

SRBC	Supercritical carbon Dioxide recompression Brayton Cycle
WHRU	Waste heat recovery unit
TC	Transcritical carbon Dioxide
VAS	Vapour Absorption System
COP	Coefficient of performance
HTR	High Temperature Regenerator
LTR	Low Temperature Regenerator
MC	Main Compressor of Supercritical carbon dioxide cycle
RC	Recompresor of Supercritical carbon dioxide cycle
TURB-1	Turbine of Supercritical carbon dioxide cycle
TURB-2	Turbine of Transcritical carbon dioxide
GEN-1	Generator of Transcritical carbon dioxide
GEN-2	Generator of vapour absorption cycle
ABS	Absorber
COND-1	Condenser of Transcritical carbon dioxide
COND-2	Condenser of Vapour absorption system
REF	Refrigerant (water) present in vapour absorption cycle
FG	Exhaust Gas
PPTD	Pinch point temperature difference

List of Content

List of Tables

List of figures

Chapter-1
Introduction

1.1 Climate change and Global Warming

The Ozone layer is a protective layer that surrounds the Earth and protects it from the sun's damaging UV radiation. This layer also aids in the maintenance of the planet's temperature, which is necessary for life to thrive. The ozone layer and the planet's equilibrium have recently shifted due to human activity. We're discussing climate change and global warming.

Planet Earth has warmed significantly over the last few decades. This is referred to as global warming, which refers to the warming of the planet, i.e., Earth. Because we live in the age of progress and capitalism, industries all around the world create dangerous pollutants. These vapours are an example of the type of material that causes ozone layer holes. These gaps allow dangerous UV rays to enter and heat the globe.

Global warming and climate change are caused by a variety of factors. The greenhouse effect is the fundamental cause of global warming and climate change. The greenhouse effect is the trapping of heat by greenhouse gases such as carbon dioxide, nitrous oxide, and others between the Ozone layer and the Earth's surface, resulting in an increase in heat as it remains trapped. As a result, the Earth's temperature continues to rise.

Greenhouse gases enter the atmosphere in a variety of ways, many of which are caused by humans. Factory fumes, smoke from automobiles and industries, and other examples of fossil fuel combustion are all contributors of global warming and climate change. Another factor is deforestation, as chopping down trees releases more carbon dioxide into the atmosphere than previously.

The melting of icecaps and glaciers throughout the planet is a by-product of climate change and global warming, raising sea levels. As a result of rising sea levels, several islands are been drowned. Heat strokes induced by heatwaves, droughts, and other extreme climatic conditions kill numerous people. Many natural catastrophes, such as forest fires, tsunamis, and floods, have been exacerbated by global warming and climate change.

Human activities are thought to have elevated Earth's global average temperature by around 1 ˚C (1.8 ˚F) since the pre-industrial period, a number that is currently increasing at a rate of 0.2 ˚C (0.36 ˚F) per decade. Human activity has unmistakably warmed the climate, oceans, and land.

To keep global warming below 2 ℃, emissions of carbon dioxide (CO2) and other greenhouse gases (GHGs) must be cut in half by 2050, according to the Intergovernmental Panel on Climate Change (IPCC) (compared with 1990 levels). Developed nations would have to decrease emissions much more – between 80-95 % by 2050 – while advanced emerging countries with substantial emissions (such as China, India, and Brazil) would have to restrict their rise in emissions.

1.2 Global energy Consumption scenario

In 2021, the world's population reached 7.63 bn, up 77 % from 4.31 bn in 1978. The worldwide (GDP) grew from 26,300 billion US dollars in 2010 to 82,645 billion US dollars in 2021. This translates to a more than threefold increase in global GDP, with an average yearly growth rate of 2.94 %.

From 270.5 EJ in 1978 to 575 EJ in 2021, worldwide primary energy consumption has more than doubled[14]. GDP per capita increased by 77.65% from 6117.8 US$2010 in 1978 to 10,900 US $2010 in 2021, while primary energy consumption climbed by 21% from 63 GJ in 1977 to 76.2 GJ in 2021. From 10.34 TJ/million US$2010 in 1978 to 7.38 TJ/million US$2010 in 2021, worldwide primary energy consumption per unit GDP decreased by 32.23 %. This equates to a 0.94 % increase in GDP's energy intensity per year.

Fossil fuels accounted for the majority of the increase in worldwide primary energy use during the last 40 years. As a result, fossil fuels' proportion of worldwide primary energy consumption was just seven %age points lower in 2021 than it was in 1978. Coal, oil, and gas still covered 84.56 % of total primary energy use in 2021.

From 18.3 billion tonnes in 1978 to 32.79 billion tonnes in 2021, worldwide energy-related CO_2 emissions climbed by 86.5 %. As a result of increased usage of nuclear and renewable energy, the carbon intensity of the world energy supply reduced from 64.43 kg CO_2/GJ in 1978 to 56.6 kg CO_2/GJ in 2021, a reduction of 13.2 %.

Recent advancements in developing technologies, energy consumption patterns, and shifting objectives in energy policy and business models indicate that the energy sector is undergoing a massive upheaval, foreshadowing the next 40 years.

1.3 Waste heat recovery potential: Indian and world scenario

A significant portion of the energy input consumed by industry, ranging from 20% to 50%, is dissipated as heat into the environment in the form of exhaust gases, waste streams of air and liquids exiting industrial facilities. For the year 2015, the industrial sector utilised 44% of total power consumption in India (1208 billion KWh), or 532 billion KWh. Even if 30% of this energy is lost by industry, this equates to 161 billion KWh a year, or the equivalent of 20000 MW of coal-fired power producing capacity. Equipment inefficiencies and thermodynamic limits of the equipment/processes are to blame for this massive quantity of waste heat. As a result, industrial facilities may decrease these losses by implementing Waste Heat Recovery system to increase the overall energy efficiency of their equipment and processes. Therefore, waste heat power generation will reduce the energy consumption per unit of production for Indian industries. Also, WHP will result in savings of fossil fuels like Diesel/ high grade coal/ furnace oil, etc. mainly used for captive power generation and thereby reducing nation's GHG emissions

With current technology, the projected waste heat power potential in the United States from industrial process heat accessible at sufficiently high temperature enough for power generation, i.e., over 300°C, is 6,000 to 8,000 MW of electricity generating capacity. The projected waste heat power potential in the United States from non-industrial process heat accessible, such as exhaust from natural gas pipeline compressor drives and landfill gas engines, is 1,000 to 2,000 MW of electric power capacity, bringing the total waste heat power potential to 7 to 10 GW. As of 2012, the total installed capacity of WHP plants in the United States was 557 MW, with WHP designated a renewable energy source in 17 US states' renewable portfolio criteria. The projected WHP capacity for the major industries in the European Union (EU) is roughly 20 TWh of electricity generation. This figure represents 4.78 % of total power usage in EU industry in 2009, implying saved CO_2 emissions of over 7.54 million tonnes. The European Union supported its first Italian prototype power plant project runs on WHP in extremely energy-intensive sectors such as steel, glass, cement, and

others, employing ORC technology with power generating sizes ranging from 0.5 to 10 MWh.

Because Indian enterprises are far less power saving than those in other sophisticated nations, there is a large potential for power generation from waste heat power in India. The industrial sector, which consumes a lot of energy, has the most potential for WHP. As of 2014, WHP-based power plants were mostly installed in cement mills across India, with a generation capacity of 79.82 MW at 11 distinct locations. Ultra tech cement has commissioned a 13.44 MW WHP plant with a capacity of 9480 TPD at Awarpur cement plants in Maharashtra. In recent years, a few waste heat power plants have now been established in the glass sector, steel industries, and so on. The following are some of the implementations of waste heat recovery systems in various industrial sectors, as well as their projected WHP capacity in India: -

Table.1.1 waste heat potential in following Indian Industries.

1	Metal casting/ foundries	152
2	Iron and steel manufacturing	789
3	Glass Manufacturing	56
4	Chemical industry	112
5	Ceramic Industry	174
6	Landfill gas energy systems	58
7	Petroleum refining (distillation/thermal cracking)	498
8	Breweries/ Food industry	252
9	Aluminium production/ Alumina industry	97
10	Pulp and paper industry	48
11	Caustic Soda	414
12	Cement Manufacturing	1105
13	Industrial boilers/ commercial sector	251
14	Natural gas compressor stations	58
15	Miscellaneous industrial sectors	1200
	Total waste heat power potential	5264

The possibility for WHP production in certain industry sectors is estimated to be over 5264 MW.

1.4 Technological Development in Waste heat Recovery for low, medium and high temperature Range

Waste heat energy is expelled from a system at a relatively high temperature to allow certain %age of the energy to be cheaply recovered for a beneficial purpose. WHP technology is Latest and established method for producing electricity affordably via process industries heat without the need of extra fossil fuels. Industrial process heat by waste heat recovery technology is converted to electrical power by sending hot exhaust gases into WHR boiler in which heat is exchanged with working fluid and afterwards expand in the turbine, forcing it to revolve and create power. In air/water cooler condenser, vapour is now condensed into low pressure vapour liquid. Unlike renewable energy sources, which are inconsistent in nature and do not provide electricity whole day, WHP can continuously create power as long as industries are running makes it a stable source of power. With recent improvements in WHR Technologies (WHRS) throughout the last decade, it has now become possible to extract electricity from process industries heat in the range of low/medium temperature, such as through the Kalina Cycle, supercritical carbon dioxide cycle (SCO_2), Organic Rankine Cycle (ORC), and others.

The temperature at which waste heat is discharged from the process/equipment can be used to classify it. The table below highlights the many types of heat sources, as well as existing WHP methods and their barriers: -

Table.1.2 Temperature based classification of waste heat potential.

Temperature Range	Heat Source	Existing Technology	Quality of waste heat

High >650 ˚C	1.Glass Melting Furnace 2.Iron Copulas 3.Coke ovens 4.Copper refining furnace 5.Cement kiln (Dry process) 6.Nickel refining furnace 7.Hydrogen Plants 8.Solid waste incinerators	Steam turbines and WHR Boilers	1.High quality of heat and transfer rate leads to more power generation and better efficiency 2.Contaminants in the heat source, both chemical and mechanical, pose a problem.
Medium 250 ˚C to 650 ˚C	1.Reciprocating Engines 2.Gas Turbine Exhaust 3.Drying Ovens 4.Baking Ovens 5.Cement Kilns 6.Catalytic Crackers 7.Steam Boiler exhaust	1.Organic Rankine cycle 2. Steam turbines and WHR Boilers 3.Kalina Cycle	1.Efficiencies of medium-power generation. 2. Mechanical and chemical impurities in heat sources like cement kilns pose a threat.
Low <250 ˚C	1.Welding Machines 2.Process steam condensate 3.Air compressors 4.IC engines 5.Air conditioning and refrigeration condensers 6.Forming dies 7.Annealing furnaces	1.Kalina Cycle 2.Organic Rankine cycle	1.Low-quality heat is stored in a large number of tiny sources, resulting in low power generation efficiency. 2. Heat recovery is limited by acid concentration in the heat source.

Chapter-2

Literature Review

Energy conservation and environmental preservation have sparked widespread concern due to a lack of energy production, low energy use efficiency, and environmental degradation. Energy supply and demand, as well as environmental issues, all play a role in the growing worldwide need for power. Alternative approaches must be used to close the gap between production and consumption. Using renewable energy sources or exhaust heat to reduce the cost of electricity generation is a critical step toward future sustainable energy and emission reduction, and improving energy efficiency can be another solution to the issue problem. As a result, it is critical to find a power generation cycle that is more efficient while using less energy.

2.1 Evolution of supercritical Carbon Dioxide Brayton cycle

At the critical point, carbon dioxide reaches the critical pressure and temperature (P_c =7.37 MPa and T_c =31.1℃). The phase state of supercritical CO_2 has a density near to liquid and a viscosity and diffusion close to gas. During the expansion phase, supercritical CO_2 exhibits gas characteristics with liquid density. Supercritical CO_2 is neither poisonous, corrosive, flammable, or explosive.

Francesco Crespi, Giacomo Gavagnin, David Sánchez, Gonzalo S. Martínez gave a comprehensive analysis of SCO_2 power cycles, spanning 42 alternative independent architectures and 38 mixed cycle combinations. These cycles have also been classified based on their primary characteristics, providing twenty-seven and thirty distinct groups. The average efficiency of the standalone cycles is around 41%. Even though oxycombustion cycles with higher turbine intake temperatures attain values in the range of 61 to 66.5 %, efficiencies in the range of 49.8 to 60.23 % appear to be possible for mixed cycle architectures [1]. Jae EunChaJoo, HyunPark, GibbeumLee, HanSeo SunilLee, Heung JuneChung, Si WooLee, in their work, optimised a pilot plant of a 504-kW supercritical CO2 power generating system for waste heat recovery employing cycle design (a basic recuperated cycle structure). Their suggested cycle attained an efficiency of 16.15 %. A compressor efficacy test was performed to ensure that the compressor was performing as expected. During the test, the compressor

operated at the design point; the compressor intake temperature was 3.5 °C at 7.6 MPa, as well as the compressor rotating speed was 34220 rpm; the compressor efficiency was 82.7 %, and the pressure ratio was 1.876[2]. Biondi, Matteo Giovanelli, Ambra Di Lorenzo, Giuseppina Salvini, Coriolano in their research integrated the SCO_2 plant with steelmaking industrial facility to assess the performance of waste heat recovery system. The waste heat recovery system design produced a total efficiency of 31.4 % and an output power of 21.16 kWe, resulting in an NPV of around US k$ 376 with a PBP of about 4.5 years [3]. Zhang, Ruiyuan Su, Wen Lin, Xinxing, Zhou Naijun, Zhao Li, under design circumstances, computed results to show that the system's energic efficiency and exergic efficiency may achieve 36.4 % and 66.40 %, respectively. Furthermore, when the high-pressure turbine's input temperature rises, cycle efficiency rises while output work falls. However, given the impact of low-pressure turbine inlet temperature, cycle efficiency as well as output work rise as temperature rises. There are pressures to achieve the highest net work as well as cycle efficiency in this system's intermediate pressure. An ideal combination of model parameters is achieved through GA optimization. The highest cycle power is 39.49 kW, and waste heat recovery efficiency may reach up to 74.63 % [4]. Khatoon, Saboora Kim, Man Hoe proposed a system that consisting the heliostat field, thermal energy storage, and the integrated carbon dioxide Brayton power cycles. The suggested system runs continuously for 24 hours, with heat transfer fluid moving between the solar receiver and storage tanks in a sinusoidal curving movement. The results show that with a recompression cycle arrangement, the linked system's efficiency is greater, with a fluctuation range of 39 to 45%. Using regeneration and recompression cycles, the computed mean net power production is 37.17 MW and 39.04 MW, respectively [5].

2.2 Integration of Supercritical Carbon Dioxide cycle with commercial cycles.

A cogeneration plant was modelled by Mojaver, Parisa Abbasalizadeh, Majid, Khalilarya, Shahram, Chitsaz that included a SOFC, a SCO_2 Brayton cycle, an ORC, and a DHR. According to the evaluation, the current density seemed to have the greatest impact on plant performance. The best condition was determined by optimization with a current density at 7880.89 A/m^2 and an anode recycle ratio of 0.478. The electrical efficiency, hot water flow rate, and CO_2 cogeneration emission

were 43.01 %, 2769 gr/s, and 213.6 kg/(MWh) in this state, respectively [6]. The research analyses Carbon dioxide power cycles with ORC, producing thermal efficacy mapping as a function of both the maximum temperature (250–650℃) and cooling qualities of varying heat inputs. The authors , Dario Alfani, Ennio Macchi[a] established that the most practical option is determined by the real boundary circumstances[7].

Yoon, S.Y.; Kim, M.J.; Kim, I.S.; Kim, T.S [8] examined the behaviour of ORC and Transcritical CO_2 cycles as a small gas turbine bottoming cycle. They demonstrate how a CO_2 recuperated cycle may outperform a basic ORC in part-load conditions. Due to the existence of the recuperator, the CO_2 recuperated cycle has a more effective heat exchange mechanism at the heat recovery unit. Nonetheless, a more extensive study that includes an ORC recuperated arrangement might be undertaken. Coconut shells had a low inorganic matter content, with a calorie content of 25.29 MJ/kg, and the highest combustion efficiency (CO2/CO) was obtained at a speed of 0.0895 $\frac{℃}{min}$ (43.16 %). The exergetic efficiency of the solar hybrid biomass SBC-ORC system was 26.60 %, up 17.28 % from the SBC-ORC/solar system in its baseline condition. The turbine inlet temperature had the biggest impact on the SBC-ORC/solar system's exergetic efficiency, which reached a high of 23.8 % at 700℃. When compared to a solo solar operation, Valencia Ochoa, G Duarte Forero [9] study showed that the unique hybrid system provides stability, superior combustion efficiency, and improved performance. The total thermodynamic efficiency and LCOE for a 100 MW cycle, according to the optimization results, were 0.521 and $52.819/MWh, accordingly. The most important indicators on the exergoeconomic performance of the triple cycle are the gas turbine inlet temperature and SCO_2 cycles. The suggested triple cycle by Mohammadi Kasra, Ellingwood Kevin, Powell Kody [10] outperforms a very thermodynamically productive cycle from the research, which featured a gas turbine topped cycle and a complicated cascade SCO_2 power cycle that employed a bottoming cycle, in terms of waste energy recovery. The suggested triple cycle provides up to 0.9 % better efficiency than the literature cycle while using less heat exchangers and turbomachinery.

2.3 Transcritical Carbon Dioxide cycle application for waste heat recovery

AlZahrani, Abdullah A Dincer, Ibrahim [11] investigated ARS with the reheat T-CO2 power cycle which has a lot of potential, especially for CSP. Variations in number of cycles pressure and temperature were explored for their impact on the power cycle's energy and exergy efficiencies, as well as integrated system efficiencies. The effects of changes in these parameters on the integrated CSP energy and exergy efficiency were also investigated. The energetic and exergetic efficiencies of the T-CO2 power cycle were 34% and 82%, accordingly. The energy and exergy efficiencies of integrated CSP (solar-to-electric) systems are roughly 20% and 55%, correspondingly. Zhang, Qiang, Ogren Ryan M Kong, Song-Charng [12] demonstrated results reveal that when compared to a gas turbine alone, the provided waste heat recovery system may enhance net power generation by 30.1 % while running at design point. The provided cycle outperforms the average cycle structure in terms of net power production and levelized energy cost, with a 5.3 % increase in net power output and a 1.2 % reduction in levelized energy cost at ideal conditions. According to the preliminary findings, the suggested CO2 power cycle offers the potential for waste heat recovery in an offshore platform application. Li, Xiaoya, Tian, Hua [13] demonstrated results indicate that CTPC systems are resilient and may safely operate even though the heat sources are very transitory, suggesting that this technology has a promising future in such applications. Furthermore, a system design that includes both a preheater as well as a recuperator appears to be the most plausible, allowing for a 2.3 % increase in brake thermal efficiency over the entire driving cycle by utilising 48.9 % of the exhaust and 72.8 % of the coolant energy, even though the pump and turbine efficiency improvements are as low as 49.75%.

2.4 Combined carbon dioxide cycle and vapour absorption refrigeration system

When compared to a standalone SCO_2 system and a combined system integrating a supercritical carbon dioxide power cycle and an absorption power cycle, the proposed system by F.Zhang, Z.chen [14] improves exergy efficiency by 9.94% and 2.80%, respectively, and reduces total product unit cost by 7.497% and 2.56 %. To recover waste heat from a marine engine, an electricity-cooling cogeneration system (ECCS) based on the connection of a steam Rankine cycle (SRC) as well as an absorption

refrigeration system (ARS) is presented by Youcai Lianga [15]. According to the simulation, retrieving the expansion work inside the absorption refrigeration cycle is indeed an efficient technique to boost power output while lowering chilling capacity. The WHR system's comparable power production is 5245 kW, accounting for 7.41 % of the marine engine's rated power output. The suggested system for engine waste heat recovery, a regeneration supercritical carbon dioxide cycle (sCO2 cycle) and an NH_3-H_2O absorption refrigeration cycle (ARC) are used by c Wu, Chuang, Xu, Xiaoxiao [16] which can improve exergy efficiency by 2.29–2.54 % point (% age point) and thermal efficiency by 8.16–18.93 % point when compared to a single regeneration supercritical carbon dioxide cycle however it may raise the overall product unit cost. The suggested system may create 248.19–253.90 kW of net output power, representing for 8.45–8.87 % of the engine's rated power output, and provide 71.57–164.6 kW of cooling load by spending 0.425–0.512 kW in pump work at varied evaporator temperatures (10–10 °C). Exergy destruction analysis also show that perhaps the elements in the bottoming ARC have lower exergy destruction rates.

Chapter-3

Description of Power cycle

In this section, an attempt was made to describe all of the relevant figures of the selected thermodynamic cycles along with their Temperature-Entropy Diagram. Focusing on the use of waste heat from a gas turbine engine's exhaust for the objective of combined power and cooling applications, a comparative analysis was performed between standalone Supercritical carbon Dioxide Brayton Cycle with recompression and proposed combined of supercritical carbon Dioxide Brayton cycle with recompression, trans critical carbon dioxide cycle and lithium bromide-Water vapour absorption system[15].

3.1 Standalone Supercritical Carbon Dioxide Brayton Cycle with Recompression

The thermodynamic performance of the recompression power cycles is greater among the different SRBC configurations in the same source of heat, and the system composition is less complex compared to others. As a result, recompression arrangement was adopted in this research.

The SRBC (supercritical CO_2 recompression Brayton cycle) is a closed Brayton cycle that uses CO_2 as the working fluid. This Brayton cycle is known as a supercritical CO_2 Brayton cycle because the working pressures and temperatures are kept above the critical point. Supercritical CO_2 recompression Brayton cycle (SRBC) described in this study consist mainly seven components- Two compressors (Main compressor and Re-compressor), a Turbine, waste heat recovery heater, precooler, low temperature regenerator (LTR) and High temperature Regenerator (HTR) etc. as shown in figure. The SRBC cycle includes the following process:

IN-OUT: Exhaust Gas of Gas turbine engine entering into the heater

5-6: Supercritical CO_2 is heated by high temperature exhaust gas in the heater

6-7: Expansion of Supercritical CO_2 in turbine-1

7-8: Supercritical CO_2 is Cooled down in High temperature Regenerator (HTR)

8-1: Supercritical CO_2 is further cooled down in Low temperature Regenerator (LTR)

1-2: Supercritical CO_2 partially enters into the Precooler and Precooled

1-4: Supercritical CO_2 Partially Enters the second compressor (called Recompressor) to increase the pressure and merge with the stream of fluid coming out of LTR at state point 4.

2-3: Partially precooled Supercritical CO_2 enter into the main compressor to increase the pressure.

3-4: Supercritical CO_2 enters the LTR and heat is gained from the stream 8-1

4-5: Supercritical CO_2 enters the HTR and heat is gained further from the stream 7-8. cycle begins again from state point 5.

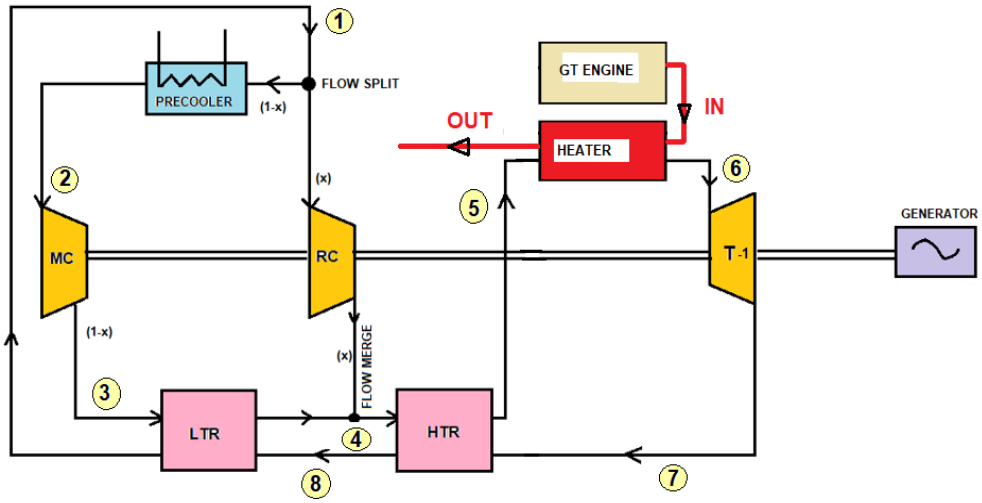

Figure 3.1 Standalone Supercritical Carbon Dioxide Recompression Brayton Cycle

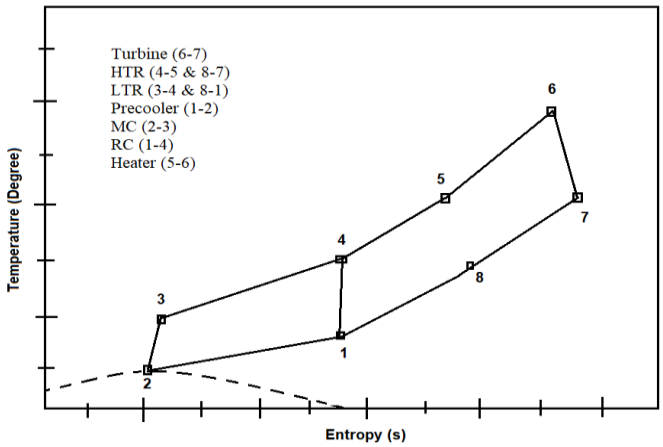

Figure 3.2 T-s Diagram of SCO_2 Recompression Brayton Cycle

3.2 Proposed combination of Supercritical Carbon Dioxide Brayton Cycle with recompression, Transcritical Carbon Dioxide Cycle and LiBr-H_2O Vapour absorption Refrigeration System.

Combination of three cycles comprised of Supercritical Carbon Dioxide Recompression Brayton cycle, Transcritical Carbon Dioxide Cycle and LiBr-H_2O Vapour absorption Refrigeration system is proposed for Both power and cooling application. Standalone supercritical Carbon Dioxide Recompression Brayton cycle has already been discussed in section 3.1. Exhaust gas will now further be utilized by addition of two more cycle. In this section working of Transcritical Carbon Dioxide Cycle and LiBr-H_2O Vapour absorption Refrigeration system will be discussed.

Transcritical carbon dioxide cycle consists of mainly four components: Turbine, condenser, Pump and a Generator. The equivalent cycle is made up of four steps, which are as follows:

9-10: High pressure Carbon Dioxide expanded into turbine-2

10-11: Carbon Dioxide enters into condenser-1 and cooled by LiBr-H_2O VAS

11-12: Low pressure Carbon Dioxide compressed in pump-1

12-9: High Pressure compressed Carbon Dioxide Exchanges Heat with Exhaust gas (28-29) and completes the cycle.

The LiBr-H_2O cycle is a type of absorption refrigeration system that uses low-grade waste heat to cool the Transcritical Carbon Dioxide cycle. LiBr-H_2O absorption Refrigeration System Processes are mentioned below:

13-14: At constant pressure, cooling is received by Transcritical CO_2 cycle from Libr-H_2O VAS in Evaporator-1/Condenser-1

14,15-16: Mixing and heat exchange with cooling water at constant pressure.

16-18: Low to High pressure process by pump-2

18-20: weak solution receives heat by strong solution at constant pressure process

20-19,21: Heat exchange by exhaust gas in generator-2 at constant pressure

21-22: Heat is transferred to cooling water at constant pressure

22-13: isenthalpic or throttling process in valve-1

19-17: constant pressure heat transfer process

17-15: isenthalpic or throttling process in valve-2

After utilization of waste heat in supercritical carbon Dioxide recompression Brayton cycle, temperature of waste heat at the exit of heater (state point 29) is still hot enough which can further be utilized by adding Transcritical Carbon Dioxide cycle and enter the Generator-1 at state point 28. While exchanging heat between state point 28-29, carbon dioxide as a working fluid (carbon dioxide) gets heated from state point 12-9. High pressure and high temperature working fluid enters the turbine hence power is generated. At state point 10, low pressure and high temperature working fluid enters the condenser-1 and receives cooling from LiBr-H_2O VAS. Cooled temperature stream at low pressure enters the Pump-1 and get pressurized till point 12. From state point 12, cycle begins again.

Temperature of waste heat exhaust at state point 29 is still hot enough which can further be utilized in LiBr-H_2O vapour absorption refrigeration system to provide cooling effect to Transcritical Carbon Dioxide cycle through Evaporator-1. In LiBr-H_2O VAS, the strong solution at state point 20 exchanges heat from the waste exhaust gas entering at state point 29 into the generator. Water (refrigerant) is removed from the weak LiBr-H_2O solution, and a strong LiBr-H_2O solution is created. The week LiBr-H_2O solution cools the strong LiBr-H_2O solution, which is throttled in a valve and delivered into the absorber. water is cooled to till saturated liquid condition in the condenser. The saturated refrigerant is throttled and delivered into the evaporator via the valve. The refrigerant is vaporised in the evaporator (13-14), creating cooling that is provided to the Transcritical Carbon Dioxide cycle. The vaporised refrigerant is then absorbed by the low temperature and low-pressure strong solution in the absorber, creating the week LiBr-H_2O solution. After being chilled by cooling water, weak solution pressure is increased by the pump and then heated in a heat exchanger by the strong LiBr-H_2O solution. Finally, the week solution is put into the generator, and the cooling cycle is completed.

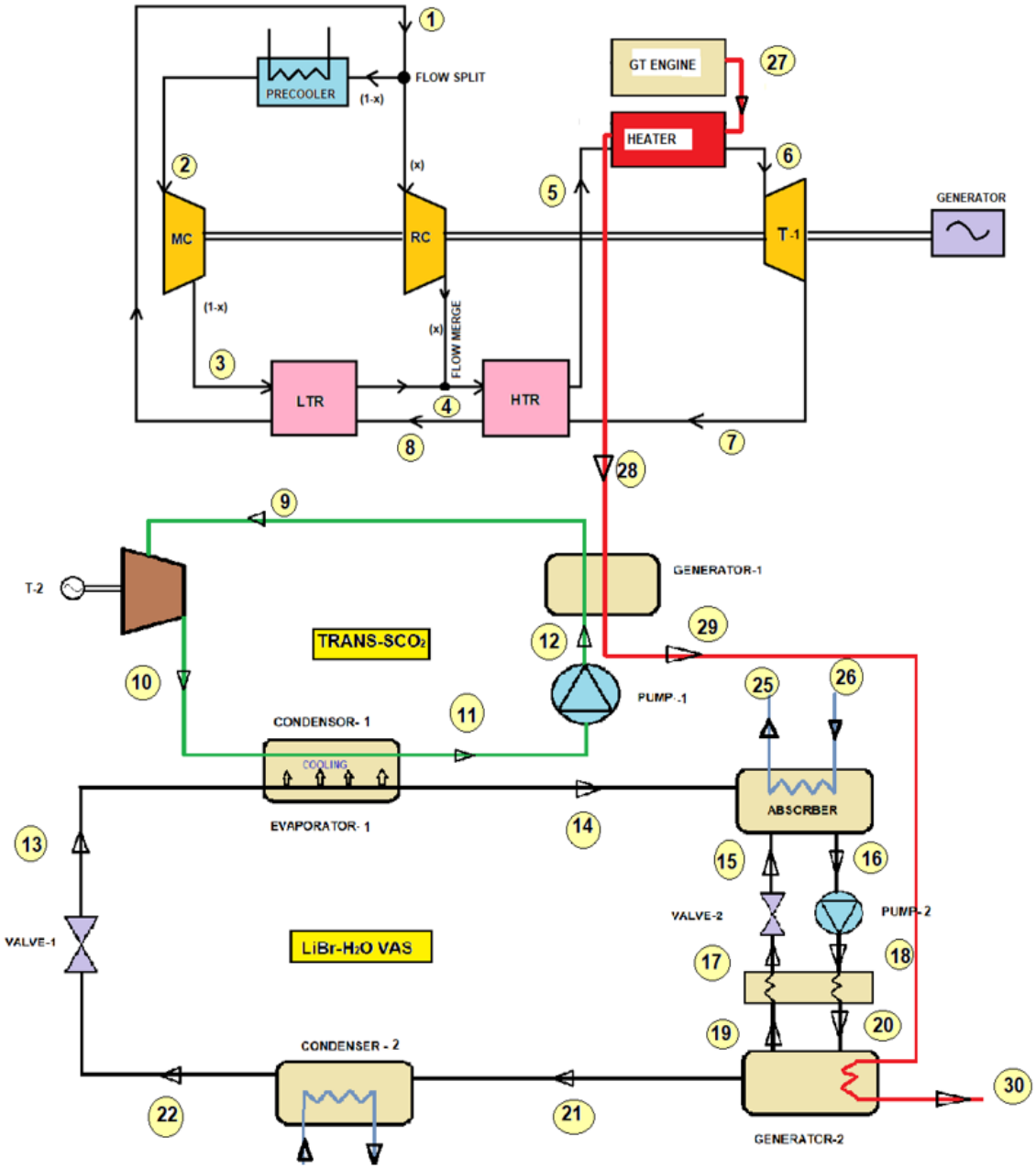

Figure 3.3 Proposed combination of SCO_2 Brayton Cycle with recompression, Transcritical CO_2 Cycle and LiBr-H_2O VAS.

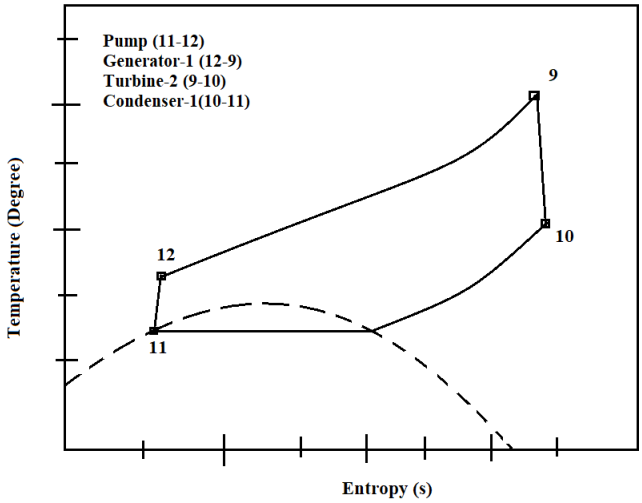

Figure 3.4 T-s Diagram of Transcritical CO_2 cycle

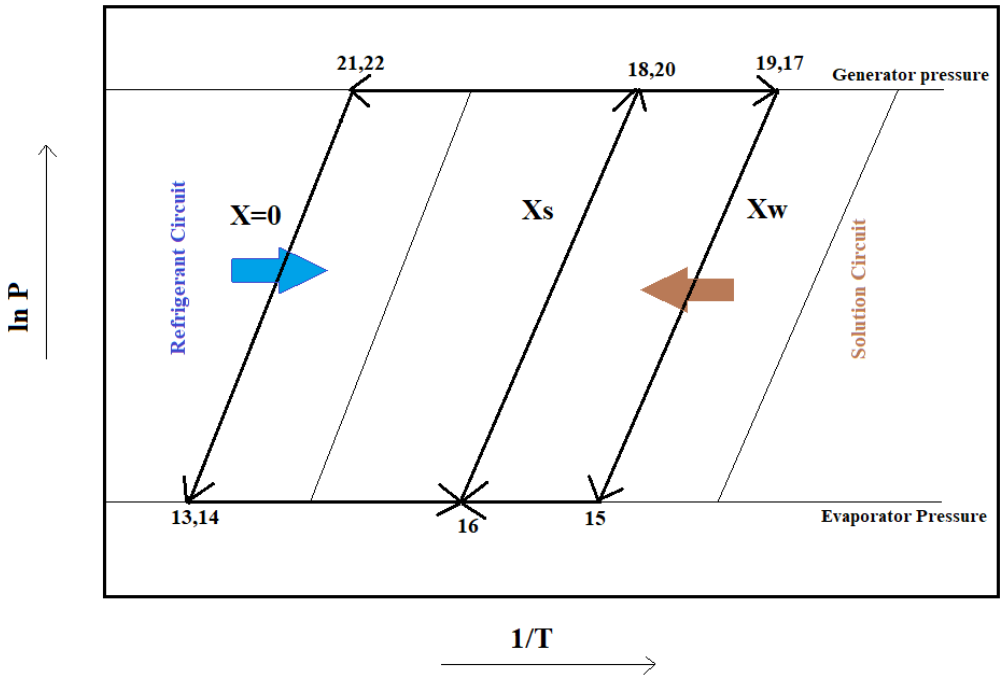

Figure 3.5 Ln P-1/T diagram for LiBr-H_2O Vapour absorption system (single effect)

3.3 Thermodynamic modelling and assessment criteria

The waste heat recovery unit (WHRU), as shown in Fig, is a combined cycle power plant that consists of a Gas turbine and proposed combined system consist of supercritical CO_2 Brayton cycle with recompression, Transcritical CO_2 cycle and LiBr-H_2O vapour absorption cycle. For thermodynamic analysis of combined system,

Titan^{TM} 350 (Designed by Solar turbines-a Caterpillar company) has been selected. Specification and performance parameters are listed below:

Table.3.1 Specification and performance parameters of Selected Gas turbine.

Parameters	**Values**
Output power	39000 kW
Heat Rate	8845 kJ/kW-hr
Exhaust Flow	371980 kg/hr
Exhaust Temperature	490 °C
Exhaust Pressure	108.4 kPa
Engine Efficiency	41%
Natural Gas fuel with LHV	35 MJ/Nm^3
Ambient Conditions	35 °C, 1 bar, 60% RH

Certain assumptions were made to make the Thermodynamic modelling and Assessment of Proposed cycle and WHRU for energy and exergy analysis easier.

1. Change in kinetic and potential energy is negligible
2. The system is in a condition of equilibrium.
3. The loss of pressure in pipes and heat exchangers is not taken into account.
4. At the condenser output, a saturated liquid condition of the working fluid is expected.
5. At ambient temperature and pressure, the cooling water enters the precooler.
6. In the pre-cooler, a temperature differential is taken into account at the pinch point.
7. In the LiBr-H_2O cycle, the outflow from the generator and the absorber are in balance.
8. Exhaust waste heat has a constant heat capacity.
9. Isentropic efficiencies are used by the turbines, compressors, and pumps.
10. Isenthalpic process takes place in throttle valves.
11. All operating fluids leak in a minimal amount.

The energy balance and mass balance equations are used to calculate and evaluate individual components and all streams in the linked system. The suggested integrated cycle was created using energic and exergic balances.

3.3.1. Supercritical CO_2 Recompression Brayton Cycle

The efficiency of the turbine-1, Main compressor and Recompresor are described as follows:

$$\eta_{s,turbine-1} = \frac{(h_6 - h_7)}{(h_6 - h_{7s})} \quad (1)$$

$$\eta_{s,MC} = \frac{(h_{3s} - h_2)}{(h_3 - h_2)} \quad (2)$$

$$\eta_{s,RC} = \frac{(h_{4s} - h_1)}{(h_4 - h_1)} \quad (3)$$

where h7s represents the enthalpy at the turbine outlet state (7s), h3s represents the enthalpy at the main-compressor outlet state (3s), and h4s represents the enthalpy at the recompression compressor outlet state (4s).[16]

The effectiveness of a heat exchanger may be stated as:

$$\varepsilon_{heater} = \frac{(T_{27} - T_{28})}{(T_{27} - T_5)} \quad (4)$$

$$\varepsilon_{HTR} = \frac{(h_7 - h_8)}{(h_7 - h_{4^*})} \quad (5)$$

$$\varepsilon_{LTR} = \frac{(h_8 - h_1)}{(h_8 - h_{3^*})} \quad (6)$$

where h_4* denotes the enthalpy of the working fluid at T = T4, P = P1; h_3* denotes the enthalpy of the working fluid at T = T3, P = P8, and it is assumed that the working fluid's minimum heat capacity is found in the high temperature streams, (2–3) in the HTR, (3–4) in the LTR, and the exhaust gas stream in the Heater.[16]

Performance of supercritical carbon dioxide recompression Brayton cycle can be evaluated using energy balance equations, based on Thermodynamics first law.

$$h_8 - h_1 = (1 - z)(h_4 - h_3) \quad (7)$$

$$h_7 - h_8 = (h_5 - h_4) \quad (8)$$

$$(1 - z)m_{co2}(h_1 - h_2) = (h_{cw1,out} - h_{cw1,in}) \quad (9)$$

$$m_{co2}(h_6 - h_5) = m_{fg}c_{p,fg}(T_{27} - T_{28}) \quad (10)$$

$$Q_{SRBC,in} = m_{co2} * (h_6 - h_5) \quad (11)$$

$$Q_{SRBC,out} = (1 - z) * m_{co2}(h_1 - h_2) \quad (12)$$

$$W_{SRBC,turbine-1} = m_{co2} * (h_6 - h_7) \quad (13)$$

$$W_{SRBC,MC} = (1 - z) * m_{co2}(h_3 - h_2) \quad (14)$$

$$W_{SRBC,RC} = z * m_{co2}(h_7 - h_4) \quad (15)$$

$$W_{SRBC,net} = W_{SRBC,turbine-1} - (W_{SRBC,MC} + W_{SRBC,RC}) \quad (16)$$

The thermal or energic efficiency of SRBC is derived from the first law of thermodynamics.

$$\eta_{I,SRBC} = \frac{W_{SRBC,net}}{Q_{SRBC,in}} \quad (17)$$

The generic equation for specific exergy flow for every state point in the cycle is calculated using the Thermodynamics second law.

$$e_i = m[(h_i - h_o) - T_o(s_{i-}s_o)] \quad (18)$$

An heat recovery cycle's exergetic efficiency is defined as the ratio of net exergy output to exergy input to the SBRC cycle through Heater.

$$\eta_{II,SRBC} = \frac{W_{SRBC,net}}{E_{SRBC,in}} \quad (19)$$

3.3.2. Transcritical Carbon Dioxide Cycle

Each stream's mass flow throughout the cycle is equal, as defined by energy consumption.

Generator-1:

$$Q_{Tc,gen-1} = m_{tco2} * (h_9 - h_{12}) \quad (20)$$

Turbine-2:

$$\eta_{s,turbine-2} = \frac{(h_9 - h_{10})}{(h_9 - h_{10s})} \quad (21)$$

$$W_{Tc,turbine-2} = m_{tco2} * (h_9 - h_{10}) \quad (22)$$

Condenser-1:

$$Q_{Tc,cond-1} = m_{tco2} * (h_{10} - h_{11}) \quad (23)$$

Pump:

$$\eta_{s,pump-1} = \frac{(h_{12s} - h_{11})}{(h_{12} - h_{11})} \quad (24)$$

$$W_{Tc,pump-1} = m_{tco2} * (h_{12} - h_{11}) \quad (25)$$

$$W_{TC,net} = W_{TC,turbine-2} - W_{Tc,pump-1} \quad (26)$$

The thermal or energic efficiency of Transcritical carbon dioxide cycle is derived from the first law of thermodynamics.

$$\eta_{I,TC} = \frac{W_{TC,net}}{Q_{Tc,gen-1}} \quad (27)$$

3.3.3. LiBr-H_2O Vapour absorption refrigeration cycle

$$Solution\ Ciculation\ Ratio(SCR) = \frac{Mass\ of\ Solution\ Leaving\ (m_s)}{Mass\ of\ absorber\ (m_r)} \quad (28)$$

Concentration, $X = \frac{mass\ of\ absorbent}{mass\ of\ solution}$ (29)

$X_{strong} = Strong\ solution\ concentration(in\ refrigent)$

$X_{weak} = Weak\ solution\ concentration(in\ refrigent)$

Absorber:

$$m_{ref} + m_{weak} = m_{strong} \quad (30)$$

$$m_{weak}X_{weak} = m_{strong}X_{strong} \quad (31)$$

$$m_{ref}h_{14} + m_{weak}h_{15} = Q_{abs} + m_{strong}h_{16} \quad (32)$$

Generator-2:

Equations 23 and 24 are similar for Generator-2

$$Q_{gen-2} + m_{strong}h_{20} = m_{ref}h_{21} + m_{weak}h_{19} \quad (33)$$

Condenser-2:

$$m_{ref}h_{21} = Q_{cond-2} + m_{ref}h_{22} \quad (34)$$

Valve-1:

$$m_{ref}h_{22} = m_{ref}h_{13} \quad \text{(Throttling)} \tag{35}$$

Evaporator-1:

$$m_{ref}h_{13} + Q_{evap-1} + m_{ref}h_{14} \tag{36}$$

Pump-2:

$$W_{pump-2} = m_{strong}(P_{18} - P_{16})v_{16} \tag{37}$$

$(P_{18} = P_{gen-2}\,, P_{16} = P_a)$

Solution heat exchanger (SHE):

$$\varepsilon_{SHE} = \frac{(T_{20} - T_{18})}{(T_{19} - T_{18})} \tag{38}$$

$$m_{strong}h_{18} + m_{weak}h_{19} = m_{strong}h_{20} + m_{weak}h_{17} \tag{39}$$

$$Q_{SHE} = m_{strong}(h_3 - h_2) = m_{weak}(h_4 - h_5) \tag{40}$$

Valve-2:

$$h_{17} = h_{15} \qquad \text{(Throttling)} \tag{41}$$

Coefficient of performance calculated for LiBr-H_2O VAS is:

$$COP_{VAS} = \frac{Q_{evap-1}}{(Q_{gen-2} + W_{pump-2})} \tag{42}$$

The thermal or energic efficiency of combined waste recovery unit is derived from the first law of thermodynamics.

$$[17]\eta_{I,overall,WHRU} = \frac{(W_{SRBC,net} + W_{TC,net} + Q_{evap-1} - W_{pump-2})}{m_{fg}c_{p,fg}(T_{27} - T_{30})} \tag{43}$$

Chapter-4

Model Validation and simulation

The thermodynamic evaluations of SCBC and Proposed cycle consist of SRBC, Transcritical Carbon dioxide cycle and LiBr-H_2O Vapour absorption refrigeration system were performed by modelling an in-house programming code written in Engineering Equation Solver (EES) software. The simulations search for state points for all cycle components employing input data based on the set of standardized operating parameters conditions shown in Table. To ensure adequate energy balance, the model includes energy and exergy balance tests. Temperature (T_a) and pressure (P_a) have been assumed to be 308.15 K (35 ℃) and 1.03 bar, respectively, for the reference condition.

Table.4.1 Standard operating condition for proposed cycle.[1][18]

Parameter	**value**	**unit**
SRBC turbine inlet temperature	468	℃
SRBC compressor inlet temperature	40	℃
SRBC maximum cycle pressure	20	MPa
SRBC minimum cycle pressure	8	MPa
pinch point temperature difference in Heater	22	℃
pinch point temperature difference in precooler	20	℃
Inlet temperature of cooling water	35	℃
SRBC isentropic efficiency of turbine	90	%
SRBC isentropic efficiency of compressor	85	%
HTR effectiveness	0.86	
LTR effectiveness	0.86	
Heater effectiveness	0.9	
TC turbine inlet temperature	200	℃
Pinch point temperature difference in Generator-1	10	℃
TC turbine isentropic efficiency	90	%
TC pump isentropic efficiency	85	%
Temperature of Evaporator-1	5	℃

Temperature of condenser-2	40	°C
Temperature of Absorber	40	°C
Temperature of Generator-2	90	°C
solution heat exchanger effectiveness	0.75	
Ambient temperature	35	°C
Ambient pressure	101.3	kPa

Chapter-5

Result and Discussion

The mathematical formulation for the comparison of Standalone Supercritical Carbon Dioxide recompression Brayton cycle (SRBC) and proposed combined of supercritical carbon Dioxide Brayton cycle with recompression, Transcritical carbon dioxide cycle and lithium bromide-Water vapour absorption system has been provided and investigated for a typical set of established parameters, as well as validated against existing literature. In the present study, special attention has been given to energic and exergic performance of standalone SRBC. For further utilization of waste heat, additional waste heat recovery cycles have been added with SRBC. Newly proposed combined cycle has been analysed based on the first law of the thermodynamics and results were compared with the standalone SRBC. Table presents the set of input data assumed, which are based upon those presented in the literature, and the results discussion follows:

5.1 Effects of pressure ratio (r_p) on the energic and exergic efficiency of SRBC

The cycle is shown to be quite responsive to the pressure ratio, and even a little deviation from of the ideal pressure ratio can result in a considerable drop in cycle performance. This pattern is due to two variables. For starters, when the pressure ratio varies, the efficacy (and consequently cycle efficiency) of heat exchangers (including HTR and LTR) is compromised due to fluctuations in the working density of the fluid, that influences pressure and velocity decreases.

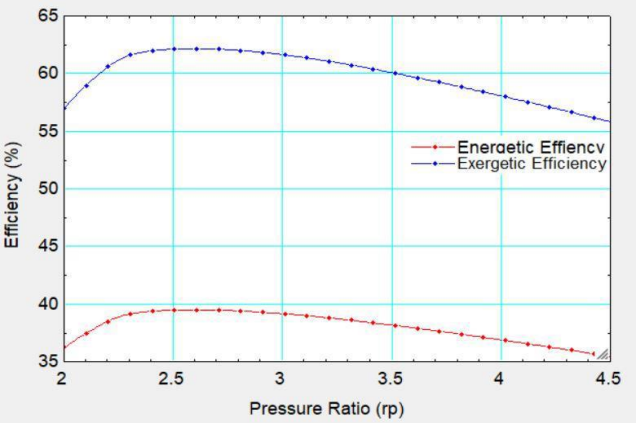

Figure 5.1. Variation of pressure ratio on the energic and exergic efficiency of SRBC.

As a result, at high pressure ratios, the density of the working medium on the larger-pressure side of heat exchangers lowers, resulting in increased velocity and pressure drops. At greater pressure ratios, the sharp increase in pressure drops with pressure ratio at the bigger pressure side of the heat exchangers, which includes HTR and LTR, adds considerably to the worsening of cycle efficiency. The HTR is responsible for the large drop in cycle efficiency for a given heat exchanger volume at low pressure ratios, while the LTR is also responsible at high pressure ratios, but to a lesser extent than the HTR.

Second, when the pressure ratio rises, the amount of heat accessible for regenerate falls, lowering total cycle efficiency.

5.2. Exergy destruction analysis of SRBC

Table.5.1 Thermodynamic properties at state point 1-8 for SRBC at standard conditions.

State point	Pressure (MPa)	Temperature (℃)	Enthalpy(kJ/kg)	Entropy(kJ/kg-K)	Exergy(kJ/kg)
1	8000	125.5	45.73	-0.6492	247.3
2	8000	40	-103.8	-1.081	230.8
3	20000	105.5	-67.91	-1.071	263.5
4	20000	221.3	120	-0.6325	316.5
5	20000	332.1	260.4	-0.3759	377.8
6	20000	468	427.1	-0.1275	467.9
7	8000	365.2	320.4	-0.1087	355.4
8	8000	241.6	179.9	-0.3532	290.3

Table.5.2 Under design settings, the SRBC energy performance

Parameters	Values	Units
Q_{Heater}	16006	kW
$Q_{precooler}$	14360	kW
$W_{SRBC,turbine-1}$	10249	kW
$W_{SRBC,MC}$	2462	kW

$W_{SRBC,RC}$	2038	kW
$W_{SRBC,net}$	5750	kW
m_{co2}	96.02	Kg/s
$\eta_{I,SRBC}$	35.92	%

Table.5.2 shows the thermodynamic parameters for SRBC under typical operating and design conditions with a cycle pressure ratio of 2.5, as illustrated in Fig. 1. Table.5.3 shows the recompression system's exergy performance under design circumstances.

Table 5.3 Under regular design settings, the recompression system's exergy performance

Components	Irreversibility (kW)	% (of total irreversibility)
Heater	887.6	23.4
HTR	359.5	9.47
LTR	498.6	13.14
Turbine	554.3	14.62
Main Compressor	220.9	5.82
Recompresor	140.6	3.7
Precooler	1131	29.82
Total irreversibility	3792.5	100
Exergy Efficiency (%)	60.26 %	

When compared to those other components, the precooler and heater have a high exergy fluctuation. The precooler has a greater exergy variation than the other components, however the RC compressor has the opposite effect, which is owing to the bigger temperature differential in the precooler. In the same way, the irreversibility of heat exchangers is shown to be substantially higher than even turbomachineries. The exergy degradation in the HTR, on the other hand, is more significant than in the LTR among regenerators. Due to the larger heat exchange temperature differential among these components, the heater, precooler, and regenerators collectively contribute around 80% of total exergy destruction within the cycle.

As a result, these subsystems are the most crucial components of a SRBC system from an exergetic standpoint.

5.3 Comparison of thermodynamic performance of proposed cycle with standalone SRBC.

Table.5.4 Thermodynamic properties at state point 9-22 for Transcritical CO_2 and LiBr-H_2O vapour absorption system at standard conditions.

State point	Pressure (MPa)	Temperature (℃)	Enthalpy(kJ/kg)	Entropy(kJ/kg-K)
9	11000	200	122	-0.5269
10	7200	161.6	92.44	-0.5193
11	7200	29.92	-204.8	-1.404
12	11000	41.62	-197.8	-1.4
13	0.8726	5	167.5	0.6029
14	0.8726	5	2510	9.024
15	0.8726	47.01	144.6	0.2746
16	0.8726	40	106.1	0.2307
17	7.381	47.01	144.6	0.2577
18	7.381	40	106.1	0.2307
19	7.381	90	224.4	0.4917
20	7.381	77.5	180.3	0.4547
21	7.381	90	2668	8.536
22	7.381	40	167.5	0.5723

Table.5.5 Under design settings, the energy performance of Transcritical CO_2 cycle

Parameters	Values	Units
$Q_{Tc,gen-1}$	14830	kW
$Q_{Tc,cond-1}$	13784	kW
$W_{Tc,turbine-2}$	1370	kW
$W_{Tc,pump-1}$	324.7	kW
$W_{TC,net}$	1045.3	kW

m_{tco2}	46.38	Kg/s
$\eta_{I,TC}$	7.04 %	%

Under typical operating and design conditions, Table.5.5 shows the thermodynamic parameters for Transcritical CO_2 with a cycle pressure ratio of 2.5, as illustrated in Fig.2.

Table.5.6 Under design settings, the energy performance of LiBr-H_2O vapour absorption system.

Parameters	Values	Units
Q_{gen-2}	18100	kW
Q_{cond-2}	14718	kW
Q_{evap-1}	13784	kW
W_{pump-2}	0.0065	kW
$Q_{absorber}$	17168	kW
m_{ref}	5.885	Kg/s
COP_{VAS}	0.7615	

Table.5.7 Under standard operating conditions, performance analysis of standalone SRBC and proposed SRBC, Transcritical Carbon dioxide and LiBr-H_2O vapour absorption system has been compared.

Efficiency	Standalone SRBC	Proposed cycle
$\eta_{thermal,overall}$	35.92 %	40.37 %
$\eta_{exergic\ SRBC}$	60.26 %	-

In this study, waste heat was introduced into SRBC. After passing through SRBC, the temperature of exhaust gas was still high enough to recover more amount of heat after. Hence, Transcritical Carbon Dioxide was introduced following SRBC to recover lower temperature part of waste heat resulting into energic efficiency of 7.04%. At the exit of TC cycle, Exhaust gas was again introduced into generator of LiBr-H_2O vapour absorption system to provide cooling, which was utilized by condenser of TC cycle to

cool the working Fluid. COP of VAS was found to be 0.7615. Hence, after series of utilization of exhaust gas through, heater of SRBC, Generator-1 of TC cycle and Generator-2 of VAS, overall efficiency of the proposed system was found to be 40.37 %.

5.4. Effects of compressor inlet temperature of SRBC.

Figure 5.2 shows that when the compressor input temperature rises, the cycle efficiency drops approximately linearly. This is due to the fact that when the compressor input temperature rises, the temperature differential between both the turbine inlet as well as the compressor reduces linearly. As a result, raising the minimum cycle temperature from 32℃ to 50℃ reduces cycle efficiency by 10.56 %, demonstrating the previously described effect of abrupt change in the specific heat capacity.

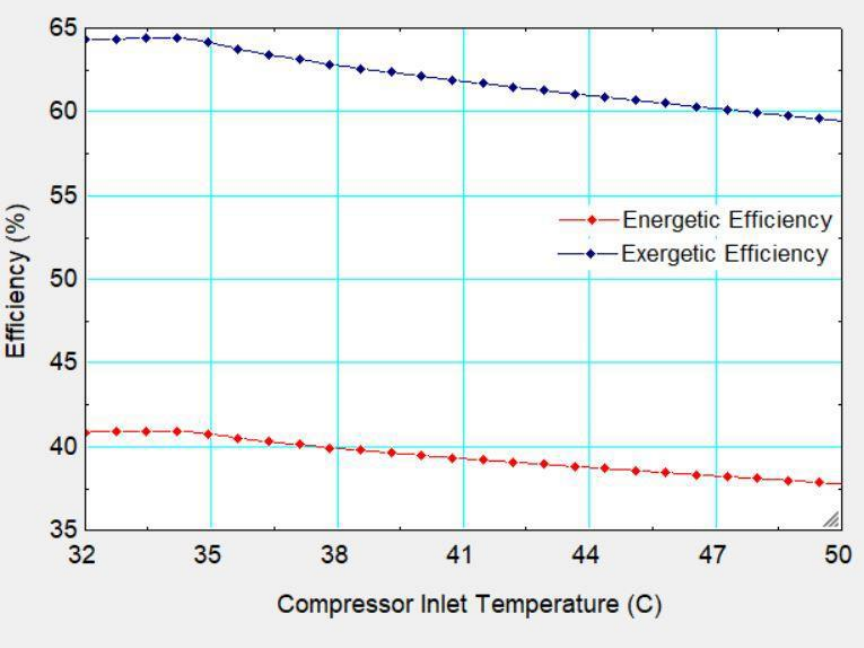

Figure 5.2. Variation of compressor inlet temperature with Energic and Exergic Efficiency of SRBC.

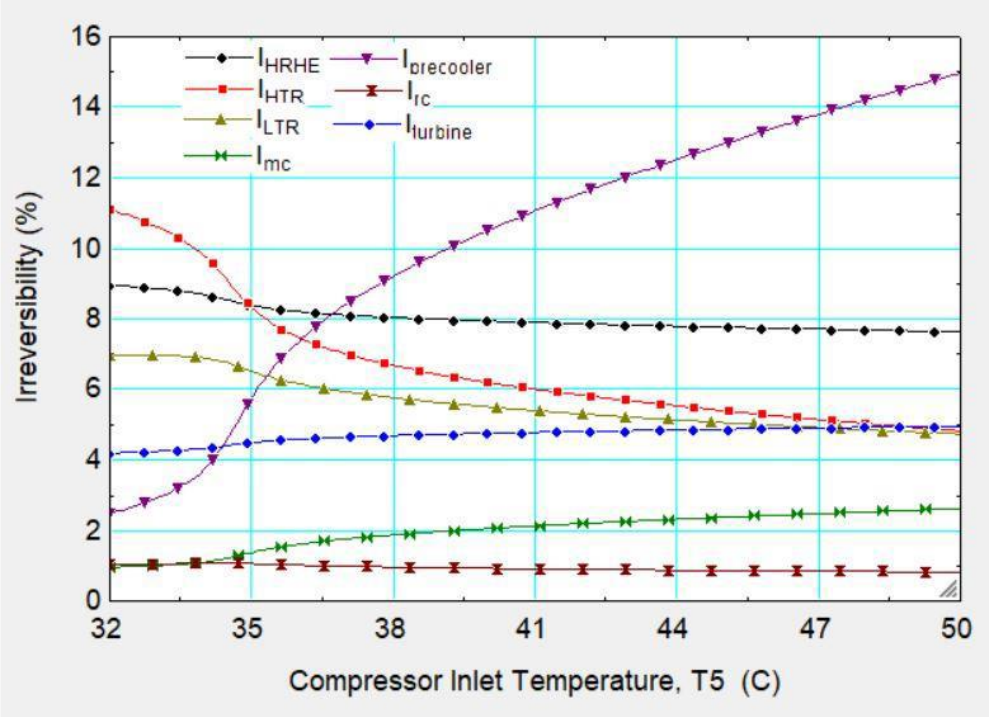

Figure 5.3. Variation of compressor inlet temperature with components irreversibility.

Figure 5.3. depicts the influence of the inlet temperature of compressor on the irreversibilities of several components for a typical set of established settings. Figure 5.2 shows that the irreversibility of the precooler grows dramatically while that of the main compressor increases just little. The abrupt fluctuations in the specific heat of a working fluid cause this particular shift in the outcome. The irreversibility of five other components, such as the Heater, LTR, turbine, and RC, however, diminishes marginally.

The physical relevance of the aforementioned findings can be interpreted in a variety of ways. Inside the case of a precooler, for example, when the temperature rises, the temperature differential between both the hot stream CO_2 as well as the cold stream (cooled water) widens, increasing the irreversibility. When the specific heat of SCO_2 degrades sufficiently distant from the critical point, it impacts heat transfer in the precooler, and hence the irreversibility rises somewhat in this area. As the mean heat transfer temperature differential (between the gas and CO_2 intake to Heater) drops as the temperature of CO_2 at Heater inlet rises alongside rise in main compressor inlet temperature, the irreversibility of a heat source (Heater) diminishes. The irreversibility inside the precooler is found to be significantly higher than those in the Heater (after

about 40 ℃) in the present study because the precooler pumping power is high due to the high mass flow rate of cooling water and high heat transfer in the precooler due to the high average heat exchange difference in temperature between CO_2 as well as the cooling water.

5.5. Effects of turbine inlet temperature of SRBC

Figure 5.4 depicts the influence of inlet temperature of turbine on efficiency. The energy and exergetic efficiency improve approximately linearly as the maximum cycle temperature rises. This is also clear since a rise in inlet temperature of turbine enhances the possibility of doing productive work. According to the thermodynamics second law, each degree increase in the temperature of the working fluid improves the quality of energy and therefore the potential to do meaningful work, i.e., the availability of the stream through the turbine, resulting in improved exergetic efficiency of the system.

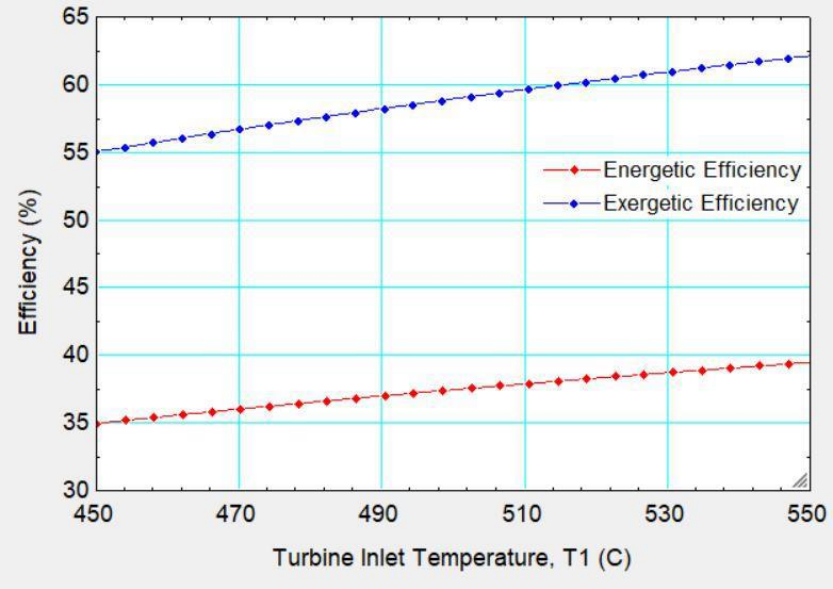

Figure 5.4. Variation of compressor inlet temperature with Energic and Exergic Efficiency of SRBC.

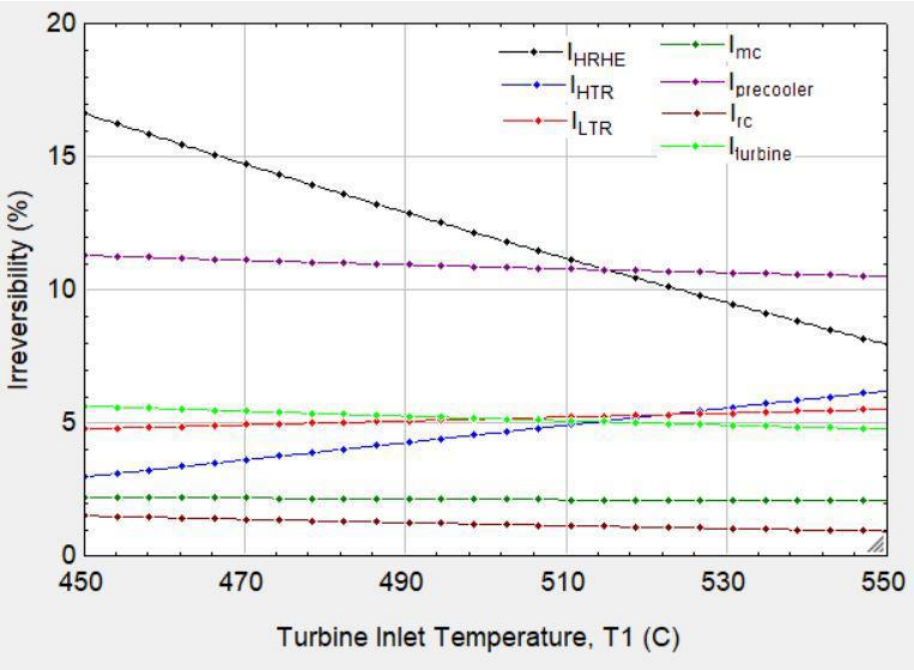

Figure 5.5. Variation of turbine inlet temperature with components irreversibility.

Furthermore, increasing the operating temperature range by 100 C increases cycle efficiency by nearly 10%, denoting that the consequence of variance as in maximum cycle temperature seems to be quite substantial, as previously discussed, due to the quality of the working medium at that specific state point.

In addition, Figure 5.5 depicts the influence of inlet temperature of turbine on component irreversibility. The irreversibility of the HRHE gradually decreases with a rise in inlet temperature of turbine, while the HTR decreases a little, as shown in Figure 5.5, because the specific heat capacity values of CO2 at all state points seem to be nearly invariant with both the rise in inlet temperature of turbine because they are located away from the critical point. As a result, all of the components[16], with the exception of the precooler and Heater, have a small impact on irreversibility. The irreversibility of the precooler, on the other side, significantly increases, while the variance in those other components like the turbine, compressors, and the LTR is essentially non-existent.

Chapter-6

Conclusion

In the present study, thermodynamic modelling and analysis of waste heat recovery comprising of Supercritical Carbon Dioxide recompression Brayton cycle, Transcritical Carbon Dioxide cycle, water lithium bromide vapour absorption system has been proposed for Gas turbine application based on first and second law thermodynamic laws. The variation of important parameters such as compressor inlet temperature, turbine inlet temperature, and pressure ratio of SRBC with energic and exergic efficiency of standalone SRBC was studied along with exergic destruction rate.

It has been found that, in comparison with turbomachinery, irreversibility of heat exchangers is higher. The precooler, Heater, and regenerators are by far the most critical components in terms of exergetic performance, according to the exergy balance. Furthermore, it is discovered that for a common set of established parameters, there may be an ideal pressure ratio where the cycle achieves maximum efficiency. Any modification in any of the operational parameters will result in a substantial change not just in the optimal pressure ratio, as well as in the cycle's thermal and exergetic efficiency. In the other words, the cycle has been discovered to be highly sensitive to the pressure ratio, and even a tiny deviation from the ideal pressure ratio can result in a considerable drop in cycle efficacy. The compressor intake temperature is shown to have a greater impact than the inlet temperature of turbine, not only on the optimal cycle pressure ratio but also in the cycle efficiency. The study clearly shows that the presence of a pressure drop causes a decrease in the stream's availability, which has a substantial effect on performance.

For now, exergic analysis has not been performed for proposed cycle which will be required to be carried out in future for betterment of Transcritical Carbon Dioxide cycle performance and higher COP of considered vapour absorption system.

REFERENCES

1. F. Crespi, G. Gavagnin, D. Sánchez, and G. S. Martínez, “Supercritical carbon dioxide cycles for power generation: A review,” Applied Energy, vol. 195. Elsevier BV, pp. 152–183, Jun. 2017. doi: 10.1016/j.apenergy.2017.02.048.
2. J. E. Cha et al., “500 kW supercritical CO2 power generation system for waste heat recovery: System design and compressor performance test results,” Applied Thermal Engineering, vol. 194. Elsevier BV, p. 117028, Jul. 2021. doi: 10.1016/j.applthermaleng.2021.117028.
3. M. Biondi, A. Giovannelli, G. Di Lorenzo, and C. Salvini, “Techno-economic analysis of a sCO2 power plant for waste heat recovery in steel industry,” Energy Reports, vol. 6. Elsevier BV, pp. 298–304, Dec. 2020. doi: 10.1016/j.egyr.2020.11.147.
4. R. Zhang, W. Su, X. Lin, N. Zhou, and L. Zhao, “Thermodynamic analysis and parametric optimization of a novel S–CO2 power cycle for the waste heat recovery of internal combustion engines,” Energy, vol. 209. Elsevier BV, p. 118484, Oct. 2020. doi: 10.1016/j.energy.2020.118484.
5. S. Khatoon and M.-H. Kim, “Preliminary design and assessment of concentrated solar power plant using supercritical carbon dioxide Brayton cycles,” Energy Conversion and Management, vol. 252. Elsevier BV, p. 115066, Jan. 2022. doi: 10.1016/j.enconman.2021.115066.
6. P. Mojaver, M. Abbasalizadeh, S. Khalilarya, and A. Chitsaz, “Co-generation of electricity and heating using a SOFC-ScCO2 Brayton cycle-ORC integrated plant: Investigation and multi-objective optimization,” International Journal of Hydrogen Energy, vol. 45, no. 51. Elsevier BV, pp. 27713–27729, Oct. 2020. doi: 10.1016/j.ijhydene.2020.07.137.
7. M. Astolfi, D. Alfani, S. Lasala, and E. Macchi, “Comparison between ORC and CO2 power systems for the exploitation of low-medium temperature heat sources,” Energy, vol. 161. Elsevier BV, pp. 1250–1261, Oct. 2018. doi: 10.1016/j.energy.2018.07.099.
8. S. Y. Yoon, M. J. Kim, I. S. Kim, and T. S. Kim, “Comparison of micro gas turbine heat recovery systems using ORC and trans-critical CO 2 cycle

focusing on off-design performance," Energy Procedia, vol. 129. Elsevier BV, pp. 987–994, Sep. 2017. doi: 10.1016/j.egypro.2017.09.223.

9. L. Meriño Stand, G. Valencia Ochoa, and J. Duarte Forero, "Energy and exergy assessment of a combined supercritical Brayton cycle-orc hybrid system using solar radiation and coconut shell biomass as energy source," Renewable Energy, vol. 175. Elsevier BV, pp. 119–142, Sep. 2021. doi: 10.1016/j.renene.2021.04.118.
10. K. Mohammadi, K. Ellingwood, and K. Powell, "A novel triple power cycle featuring a gas turbine cycle with supercritical carbon dioxide and organic Rankine cycles: Thermoeconomic analysis and optimization," Energy Conversion and Management, vol. 220. Elsevier BV, p. 113123, Sep. 2020. doi: 10.1016/j.enconman.2020.113123.
11. A. AlZahrani and I. Dincer, "Thermodynamic analysis of an integrated transcritical carbon dioxide power cycle for concentrated solar power systems," Solar Energy, vol. 170. Elsevier BV, pp. 557–567, Aug. 2018. doi: 10.1016/j.solener.2018.05.071.
12. Q. Zhang, R. M. Ogren, and S.-C. Kong, "Thermo-economic analysis and multi-objective optimization of a novel waste heat recovery system with a transcritical CO2 cycle for offshore gas turbine application," Energy Conversion and Management, vol. 172. Elsevier BV, pp. 212–227, Sep. 2018. doi: 10.1016/j.enconman.2018.07.019.
13. X. Li, H. Tian, G. Shu, M. Zhao, C. N. Markides, and C. Hu, "Potential of carbon dioxide transcritical power cycle waste-heat recovery systems for heavy-duty truck engines," Applied Energy, vol. 250. Elsevier BV, pp. 1581–1599, Sep. 2019. doi: 10.1016/j.apenergy.2019.05.082.
14. T. Kober, H.-W. Schiffer, M. Densing, and E. Panos, "Global energy perspectives to 2060 – WEC's World Energy Scenarios 2019," Energy Strategy Reviews, vol. 31. Elsevier BV, p. 100523, Sep. 2020. doi: 10.1016/j.esr.2020.100523.
15. C. Wu, X. Xu, Q. Li, J. Li, S. Wang, and C. Liu, "Proposal and assessment of a combined cooling and power system based on the regenerative supercritical carbon dioxide Brayton cycle integrated with an absorption refrigeration cycle for engine waste heat recovery," Energy Conversion and Management, vol.

207. Elsevier BV, p. 112527, Mar. 2020. doi: 10.1016/j.enconman.2020.112527.

16. O. P. Sharma, S. C. Kaushik, and K. Manjunath, “Thermodynamic analysis and optimization of a supercritical CO2 regenerative recompression Brayton cycle coupled with a marine gas turbine for shipboard waste heat recovery,” Thermal Science and Engineering Progress, vol. 3. Elsevier BV, pp. 62–74, Sep. 2017. doi: 10.1016/j.tsep.2017.06.004.
17. M. Altinkaynak and M. Ozturk, “Thermodynamic analysis of a novel integrated system operating with gas turbine, s-CO2 and t-CO2 power systems for hydrogen production and storage,” International Journal of Hydrogen Energy, vol. 47, no. 5. Elsevier BV, pp. 3484–3503, Jan. 2022. doi: 10.1016/j.ijhydene.2021.07.212.
18. S. Yang, C. Deng, and Z. Liu, “Optimal design and analysis of a cascade LiBr/H2O absorption refrigeration/transcritical CO2 process for low-grade waste heat recovery,” Energy Conversion and Management, vol. 192. Elsevier BV, pp. 232–242, Jul. 2019. doi: 10.1016/j.enconman.2019.04.045.
19. Z. Su et al., “Opportunities and strategies for multigrade waste heat utilization in various industries: A recent review,” Energy Conversion and Management, vol. 229. Elsevier BV, p. 113769, Feb. 2021. doi: 10.1016/j.enconman.2020.113769.
20. M. Pan et al., “4E analysis and multiple objective optimizations of a cascade waste heat recovery system for waste-to-energy plant,” Energy Conversion and Management, vol. 230. Elsevier BV, p. 113765, Feb. 2021. doi: 10.1016/j.enconman.2020.113765.
21. T. Ni, J. Si, F. Lu, Y. Zhu, and M. Pan, “Performance analysis and optimization of cascade waste heat recovery system based on transcritical CO2 cycle for waste heat recovery in waste-to-energy plant,” Journal of Cleaner Production, vol. 331. Elsevier BV, p. 129949, Jan. 2022. doi: 10.1016/j.jclepro.2021.129949.
22. B. Patel, N. B. Desai, and S. S. Kachhwaha, “Optimization of waste heat based organic Rankine cycle powered cascaded vapor compression-absorption refrigeration system,” Energy Conversion and Management, vol. 154. Elsevier BV, pp. 576–590, Dec. 2017. doi: 10.1016/j.enconman.2017.11.045.

23. K. Manjunath, O. P. Sharma, S. K. Tyagi, and S. C. Kaushik, “Thermodynamic analysis of a supercritical/transcritical CO 2 based waste heat recovery cycle for shipboard power and cooling applications,” Energy Conversion and Management, vol. 155. Elsevier BV, pp. 262–275, Jan. 2018. doi: 10.1016/j.enconman.2017.10.097.
24. Waste heat power Generation as new source of energy, Ministry of New and Renewable Energy (Government of India).
25. Y. Liang, Z. Sun, M. Dong, J. Lu, and Z. Yu, “Investigation of a refrigeration system based on combined supercritical CO2 power and transcritical CO2 refrigeration cycles by waste heat recovery of engine,” International Journal of Refrigeration, vol. 118. Elsevier BV, pp. 470–482, Oct. 2020. doi: 10.1016/j.ijrefrig.2020.04.031.
26. N. Georgousis, P. Lykas, E. Bellos, and C. Tzivanidis, “Multi-objective optimization of a solar-driven polygeneration system based on CO2 working fluid,” Energy Conversion and Management, vol. 252. Elsevier BV, p. 115136, Jan. 2022. doi: 10.1016/j.enconman.2021.115136.
27. A. Yu, W. Su, X. Lin, and N. Zhou, “Recent trends of supercritical CO2 Brayton cycle: Bibliometric analysis and research review,” Nuclear Engineering and Technology, vol. 53, no. 3. Elsevier BV, pp. 699–714, Mar. 2021. doi: 10.1016/j.net.2020.08.005.
28. Y. Ma, X. Zhang, M. Liu, J. Yan, and J. Liu, “Proposal and assessment of a novel supercritical CO2 Brayton cycle integrated with LiBr absorption chiller for concentrated solar power applications,” Energy, vol. 148. Elsevier BV, pp. 839–854, Apr. 2018. doi: 10.1016/j.energy.2018.01.155.
29. J. Yuan, C. Wu, X. Xu, and C. Liu, “Proposal and thermoeconomic analysis of a novel combined cooling and power system using carbon dioxide as the working fluid,” Energy Conversion and Management, vol. 227. Elsevier BV, p. 113566, Jan. 2021. doi: 10.1016/j.enconman.2020.113566
30. P. Mojaver, M. Abbasalizadeh, S. Khalilarya, and A. Chitsaz, “Co-generation of electricity and heating using a SOFC-ScCO2 Brayton cycle-ORC integrated plant: Investigation and multi-objective optimization,” International Journal of Hydrogen Energy, vol. 45, no. 51. Elsevier BV, pp. 27713–27729, Oct. 2020. doi: 10.1016/j.ijhydene.2020.07.137.